Eur. Phys. J. A **31**, 141–154 (2007)
DOI 10.1140/epja/i2006-10153-2

THE EUROPEAN PHYSICAL JOURNAL A

Regular Article – Nuclear Structure and Reactions

Low-spin states in ^{182}Os and $K^\pi = 0^+, 2^+$ excited bands

M.A. Cardona[1,2,3,4,a], D. Hojman[1,2,3], B. Roussière[2], J. Libert[2], J. Genevey[5], J. Sauvage[2], and the ISOCELE and ISOLDE Collaborations

[1] Departamento de Física, Comisión Nacional de Energía Atómica, Buenos Aires, Argentina
[2] Institut de Physique Nucléaire, IN2P3-CNRS/Université Paris-Sud, F-91406 Orsay Cedex, France
[3] CONICET, Buenos Aires, Argentina
[4] Escuela de Ciencia y Tecnología, Universidad de San Martín, Argentina
[5] Laboratoire de Physique Subatomique et de Cosmologie, IN2P3-CNRS/Université Joseph Fourier, F-38026 Grenoble Cedex, France

Received: 18 October 2006
Published online: 6 February 2007 –
Communicated by J. Äystö

Abstract. Excited states in ^{182}Os were populated by the β^+/EC decay of ^{182}Ir following mass separation. Gamma-ray and conversion electron spectroscopy techniques were employed. Monopole ($E0$) contributions were determined in transitions populating the ground-state band. A systematic study of the low-spin structures in the Os isotopes is presented and a detailed analysis in the framework of a microscopic configuration mixing approach is performed.

PACS. 21.10.Hw Spin, parity, and isobaric spin – 23.20.Lv γ transitions and level energies – 23.20.Nx Internal conversion and extranuclear effects – 27.70.+q $150 \leq A \leq 189$

1 Introduction

In the last few years, experimental data and complete systematic studies focused on the non-yrast collective structures of even-even W, Os and Pt nuclei have been published including data of the ^{182}Os nucleus [1–3]. In addition, the ^{182}Os nucleus has been extensively studied by heavy-ion–induced reactions [4]. However, in the investigations of ^{182}Os through β^+/EC decay a lot of transitions remained unplaced, involving a large amount of unplaced intensity [4]. Here we present new experimental results of the ^{182}Ir β^+/EC decay studies. An interesting characteristic of this mass region is the existence of unusual highly converted transitions not only in even-even but also in odd-A nuclei [5], that have been explained in terms of an $E0$ component in the transition or an $M1$ conversion anomaly. In the case of transitions populating levels of the ground-state band in even-even nuclei (considered as almost pure $K^\pi = 0^+$ band), $E0$ components indicate that the initial states contain $K^\pi = 0^+$ components, since $E0$ transitions imply $\Delta K = 0$, $\Delta I = 0$, and $\Delta\pi = +$. In the present work several highly converted transitions have been found in ^{182}Os which were used to identify possible $K^\pi = 0^+$ excitations. In particular, among the lowest collective excitations in deformed even-even nuclei the first excited $K^\pi = 0^+$ bands have traditionally been described as β vibrations. However, further investigations have revealed properties of these $K^\pi = 0^+$ states which require other characterizations [6,7]. We present also a detailed analysis of the large amount of experimental information available on the Os isotopes using dynamical calculations (Generator Coordinate Method under Gaussian Overlap Approximation) based on Hartree-Fock-Bogoliubov (HFB) states obtained with the D1S Gogny's force [8]. In this theoretical framework we calculate energy levels and electromagnetic properties in an attempt to characterize some of the low-spin excited states observed in the ^{182}Os nucleus.

2 Experimental measurements

The present ^{182}Os results have been obtained as by-product of two experiments devoted to the ^{182}Pt $\rightarrow$ ^{182}Ir decay study. In both experiments, excited levels in ^{182}Os were populated by the β^+/EC decay of the ^{182}Ir nucleus ($T_{1/2} = 15$ m). In the first experiment the ^{182}Ir nuclei were produced by two successive β^+/EC decays of ^{182}Au. The gold isotopes were obtained in the Pt(p, xn)Au reaction. The target consisted of a 7 g Pt-B alloy placed inside the ion source of the ISOCELE separator [9,10] and was bombarded with a 200 MeV proton beam provided by the Orsay synchrocyclotron. The mass-separated ra-

[a] e-mail: cardona@tandar.cnea.gov.ar

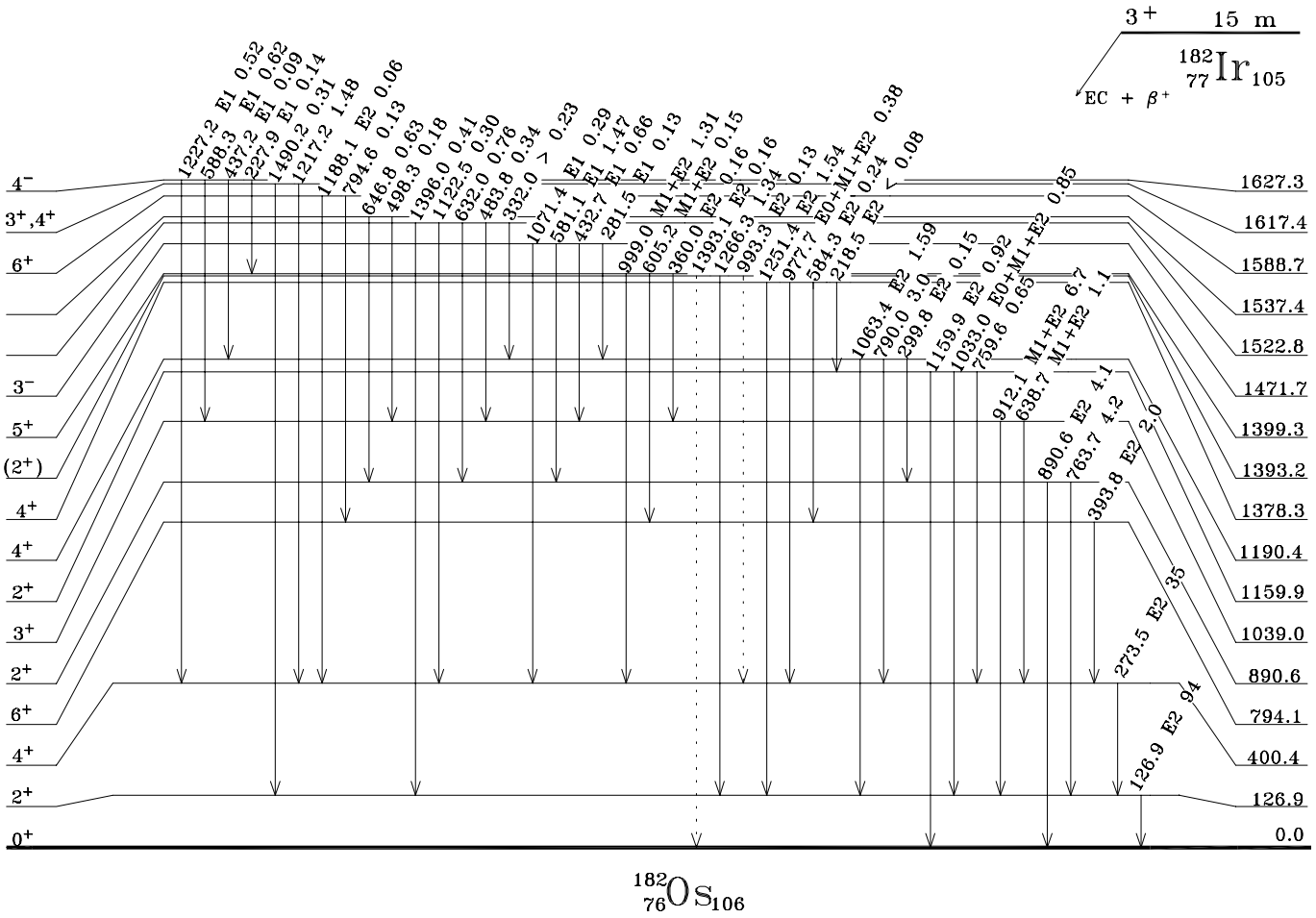

Fig. 1. Level scheme for ^{182}Os from ^{182}Ir decay (lower part). Total intensities, $I(\gamma + ce)$, per 100 parent decays and some multipolarities are indicated.

dioactive sources of ^{182}Au were collected during 200 s on an aluminized-mylar tape and, after 100 s of waiting time, moved to the detection setup and measured during 300 s. The counting system consisted of two coaxial and one planar X-ray Ge(HP) detectors covering an energy range from 12 to 2700 keV. Singles γ-spectra were measured for the three detectors and three types of double coincidences were recorded in event-by-event mode on a magnetic tape. The recorded data were sorted into prompt and delayed coincidence two-dimensional matrices. A second radioactive decay experiment focused on conversion electron measurements was performed at ISOLDE/CERN [11]. In this experiment, the ^{182}Ir nuclei were obtained as descendant of ^{182}Hg nuclei by successive β^+/EC decays. The mercury isotopes were produced by bombarding a molten lead target [12] with a 1 GeV proton beam delivered by the CERN PS Booster. The target was connected to a hot plasma ion source and the extracted ion beam was mass-separated by ISOLDE. The cycle was chosen with a collection time of 15 s, a waiting time of 115 s, and a counting time of 130 s. In both experiments the cycle times were chosen to favor the ^{182}Pt ($T_{1/2} = 2.6$ m) decay in the radioactive $A = 182$ chain, since, as mentioned before, the main purpose of the experiments was the study of ^{182}Ir. The radioactive nuclei were implanted onto an aluminized mylar tape and moved to the detection system for the e^--γ experiment which consisted of a cooled 3 mm thick Si(Li) detector for electron detection and a coaxial Ge(HP) gamma detector. Singles spectra and e^--γ coincidence events were recorded covering an energy range up to 1.5 MeV.

3 Experimental results

The level scheme of ^{182}Os built from the β^+/EC decay of ^{182}Ir in this work is presented in two parts, in figs. 1 and 2. A total of 81 transitions were placed in the level scheme, extending widely the previous known decay scheme [4], eighteen new levels have been established. The assignment of new lines to ^{182}Os was based on coincidence with the Os X-rays and with known transitions of this nucleus. Among the new levels established in this β^+/EC decay work two of them were known from high-spin studies: the 5^- states located at 1735.1 and 1895.3 keV [4]. The energy, γ-ray intensity, location, and main coincidences of the transitions assigned to the ^{182}Ir $\rightarrow$ ^{182}Os decay are listed in

Table 1. Gamma-ray data for the ^{182}Ir → ^{182}Os decay.

E_γ^a (keV)	I_γ^b	$E_i \rightarrow E_f$ (keV) (keV)	Main coincident γ-rays (keV)
126.9	1110(36)	126.9 → 0.0	274,394,764,790,912,999,1063,1217,1251,1266
159.2	4.5(12)	1813.3 → 1654.1	127,182,274,581,860,1254
182.3	13.3(18)	1654.1 → 1471.7	127,159,274,433,581,764,891,912,1071
197.6	4.5(11)^c	1669.4 → 1471.7	127,274,581,764,891,912
218.5	$\leq 2^c$	1378.3 → 1159.9	1033,1160
227.9	4.3(9)	1627.3 → 1399.3	127,274,999
249.1	9.8(13)	1876.3 → 1627.3	127,274,588,912
254.7	3.7(13)	1654.1 → 1399.3	127,274,999
273.5	1000(22)	400.4 → 126.9	127,394,639,760,790,978,999,1071,1123,1217,1227,1254,1269
281.5	4.0(10)^c	1471.7 → 1190.4	127,274,790
299.8	4.4(8)	1190.4 → 890.6	127,764,891
332.0	7.3(10)	1522.8 → 1190.4	127,274,790,1063
360.0	4.8(15)^c	1399.3 → 1039.0	127,912
386.1	2.5(8)^c	1785.5 → 1399.3	127,274,999
393.8	62.6(23)	794.1 → 400.4	127,274,584,605,795,860,941,1101
405.4	4.9(11)^c	2059.5 → 1654.1	127,182,274,581
432.7	21.1(16)	1471.7 → 1039.0	127,182,274,639,912
437.2	2.8(8)^c	1627.3 → 1190.4	127,274,790
450.8	10(2)	1640.9 → 1190.4	127,274,790,1063
478.9	5.5(9)	1669.4 → 1190.4	127,274,790,1063
483.8	11.0(15)	1522.8 → 1039.0	127,274,639,912
498.3	5.7(14)	1537.4 → 1039.0	127,912
544.4	10.9(11)	1735.1 → 1190.4	127,274,790,1063
581.1	47.2(2.7)	1471.7 → 890.6	127,182,764,891
584.3	7.6(15)^c	1378.3 → 794.1	127,274,394
588.3	20.0(20)^c	1627.3 → 1039.0	127,274,639,912
595.1	6.3(10)	1785.5 → 1190.4	127,274,790,1063
601.7	10.1(14)	1640.9 → 1039.0	127,274,639,912
605.2	4.7(10)	1399.3 → 794.1	127,274,394
630.2	5.4(8)^c	1669.4 → 1039.0	127,912
632.0	24.3(27)	1522.8 → 890.6	127,764,891
638.7	35.1(18)	1039.0 → 400.4	127,274,433,484,588,602,746,837
646.8	20.3(21)^c	1537.4 → 890.6	127,764,891
705.2	3.1(8)^c	1895.3 → 1190.4	127,274,790
746.2	9.5(10)^c	1785.5 → 1039.0	127,274,639,912
750.2	12.5(13)	1640.9 → 890.6	127,764,891
759.6	20.7(15)	1159.9 → 400.4	127,274
763.7	136(5)	890.6 → 126.9	127,182,581,632,647,750,1009,1135
790.0	96(5)^c	1190.4 → 400.4	127,274,282,332,437,451,479,544
794.6	4.1(10)^c	1588.7 → 794.1	127,274,394
837.3	9.0(8)	1876.3 → 1039.0	127,274,639,912
860.0	5.2(8)	1654.1 → 794.1	127,159,274,394
875.8	1.8(5)^c	1669.4 → 794.1	127,274,394
890.6	132(5)	890.6 → 0.0	182,581,632,647,750,1009,1135
912.1	215(7)	1039.0 → 126.9	127,360,433,484,498,588,602,630,746,837,986
941.2	3.0(8)	1735.1 → 794.1	127,274,394
977.7	12.2(11)	1378.3 → 400.4	127,274
985.7	4.2(9)	2025.1 → 1039.0	127,912
993.3	4.0(12)^c	1393.2 → 400.4	(127),274
999.0	42.0(20)	1399.3 → 400.4	127,228,255,274,386
1008.6	3.9(7)	1899.3 → 890.6	127,764,891
1033.0	27.1(12)	1159.9 → 126.9	127
1063.4	51.0(20)	1190.4 → 126.9	127,282,332,451,479,544
1071.4	9.2(7)	1471.7 → 400.4	127,182,274
1101.2	2.6(7)^c	1895.3 → 794.1	127,274,394
1122.5	9.6(15)	1522.8 → 400.4	127,274
1134.8	5.1(10)	2025.1 → 890.6	127,764,891

Table 1. Continued.

E_γ^a (keV)	I_γ^b	$E_i \rightarrow E_f$ (keV) (keV)	Main coincident γ-rays (keV)
1159.9	29.5(14)	1159.9 → 0.0	
1188.1	1.9(7)[c]	1588.7 → 400.4	127,274
1217.2	47.4(23)	1617.4 → 400.4	127,274
1227.2	16.6(10)	1627.3 → 400.4	127,274
1240.6	5.0(8)	1640.9 → 400.4	127,274
1251.4	49.5(20)	1378.3 → 126.9	127
1253.6	11.1(10)	1654.1 → 400.4	127,274
1266.3	42.9(25)	1393.2 → 126.9	127
1269.2	4.3(11)	1669.4 → 400.4	127,274
1334.5	5.9(20)	1735.1 → 400.4	127,274
1353.5	5.0(13)	2147.5 → 794.1	127,274,394
1374.8[d]	4.0(8)		127,274
1385.4	6.3(10)	1785.5 → 400.4	127,274
1393.1	5.0(13)	1393.2 → 0.0	
1396.0	13.0(20)	1522.8 → 126.9	127
1444.1	15.6(15)	1844.5 → 400.4	127,274
1490.2	10.0(10)	1617.4 → 126.9	127
1495.0	1.5(7)	1895.3 → 400.4	127,274
1498.9	9.2(9)	1899.3 → 400.4	127,274
1514.0	11.3(11)	1640.9 → 126.9	127
1549.7	15.8(16)	1676.6 → 126.9	127
1575.6[d]	7.2(11)		127,274
1642.0	16.8(9)	1768.9 → 126.9	127
1651.0[d]	4.6(6)		127,274
1662.3[d]	6.0(6)		127,274
1676.7	3.9(15)	1676.6 → 0.0	
1722.8[d]	9.3(14)		127,274
1747.1	8.3(13)	2147.5 → 400.4	127,274
1769.0	8.0(11)	1768.9 → 0.0	

[a] Uncertainties between 0.1 and 0.3 keV.

[b] Normalization taken as $I_\gamma(273.5\,\text{keV}) = 1000$.

[c] γ-ray intensity estimated from coincidence spectra.

[d] Transition assigned to ^{182}Os but not placed in the level scheme.

table 1. We also report in table 1 weak γ-rays observed in coincidence with the strong transitions of the ground-state band and not placed in the level scheme. The γ-ray intensities reported in table 1 were evaluated in the first of the experiments described in the previous section, using singles spectra except for some weak or contaminated transitions for which coincidence data were used. The efficiency calibration of the gamma detectors was performed using standard ^{133}Ba and ^{152}Eu sources and was internally checked in the coincidence spectrum gated on the 393.8 keV line, where the total intensities of the 126.9 and 273.5 keV transitions are equal within their error bars. In addition, in the level scheme (figs. 1 and 2) we report the total intensities per 100 parent decays; these values were obtained from the γ-ray intensities of table 1 and the total internal conversion coefficients evaluated using the HSICC code [13]. For transitions of energy greater than 400 keV the conversion electron contribution was neglected. In the case of some low-energy transitions of unknown multipolarity (159.2, 249.1, 332.0, and 386.1 keV) a lower limit of the total intensity, which corresponds to the γ-ray intensity, is reported. Some multipolarities are also indicated in figs. 1 and 2. Representative gated coincidence spectra are shown in figs. 3 and 4. In fig. 3(b) the weak transitions of 1269.2, 1334.5 and 1385.4 keV all of them with γ-ray intensity less than 8 in table 1 are clearly seen in coincidence with the 273.5 keV γ-ray. In figs. 4 (a) and (b) the following pairs of transitions: (750.2 and 601.7 keV), (646.8 and 498.3 keV) and (632.0 and 483.8 keV), which depopulate the new levels at 1640.9, 1537.4 and 1522.8 keV, respectively, are clearly observed. The 1393.1, 1676.7 and 1769.0 keV transitions are indicated by dashed lines in the level scheme (figs. 1 and 2) since their energies fit well with level energies of the scheme but their placements could not be supported by coincidence relationships. They correspond to lines remained unassigned in the singles spectra, and strong enough to discard the possibility of being sum peaks (including the 126.9 keV line). The 993.3 keV transition is also represented by a dashed line because it is observed only in coincidence with the 273.5 keV line, and the coincidence with the 126.9 keV ray is strongly dependent on the background subtraction. Other three transitions,

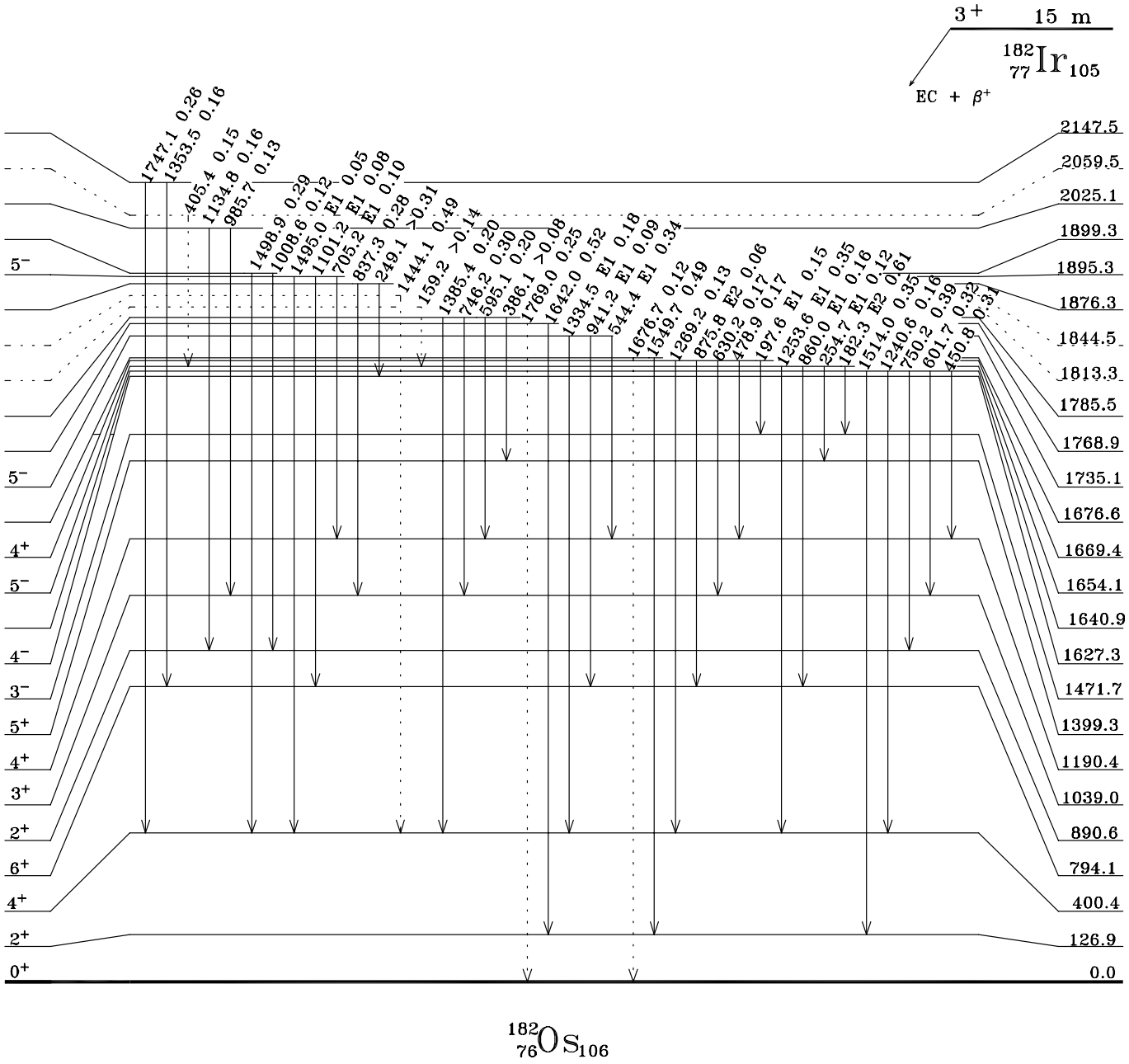

Fig. 2. Level scheme for ^{182}Os from ^{182}Ir decay (higher part). Total intensities, $I(\gamma + ce)$, per 100 parent decays and some multipolarities are indicated.

the 159.2, 405.4, and 1444.1 keV lines, which depopulate levels not fixed by additional decays, are also indicated by dashed lines.

Our results are basically in agreement with those presented in ref. [2] except for some differences in the γ-ray intensities. For example, in the present work, the γ-ray intensity of the 126.9 keV $2^+ \rightarrow 0^+$ transition relative to the 273.5 keV $4^+ \rightarrow 2^+$ transition is around 40% larger than the value reported by Kibédi *et al.* [2]. Moreover, we found systematically larger (smaller) γ-ray intensities (relative to the 273.5 keV intensity) for transitions de-exciting levels with spin value $\leq$ ($>$)4 than those given in ref. [2]. All this seems to indicate that our γ-ray intensity values are systematically higher for transitions de-exciting levels that could be directly populated in the β^+/EC decay of ^{182}Ir. This conclusion is supported by the fact that in ref. [2] for the ^{182}Os study, γ-γ coincidence measurements are reported but no singles γ-ray measurements. Moreover, our γ-ray intensity values are in quite good agreement with the results from the earlier radioactivity studies [14–16], except for the 126.9 keV transition that we found more intense. However, as indicated above, we have measured the detector efficiency very accurately, especially at low energy.

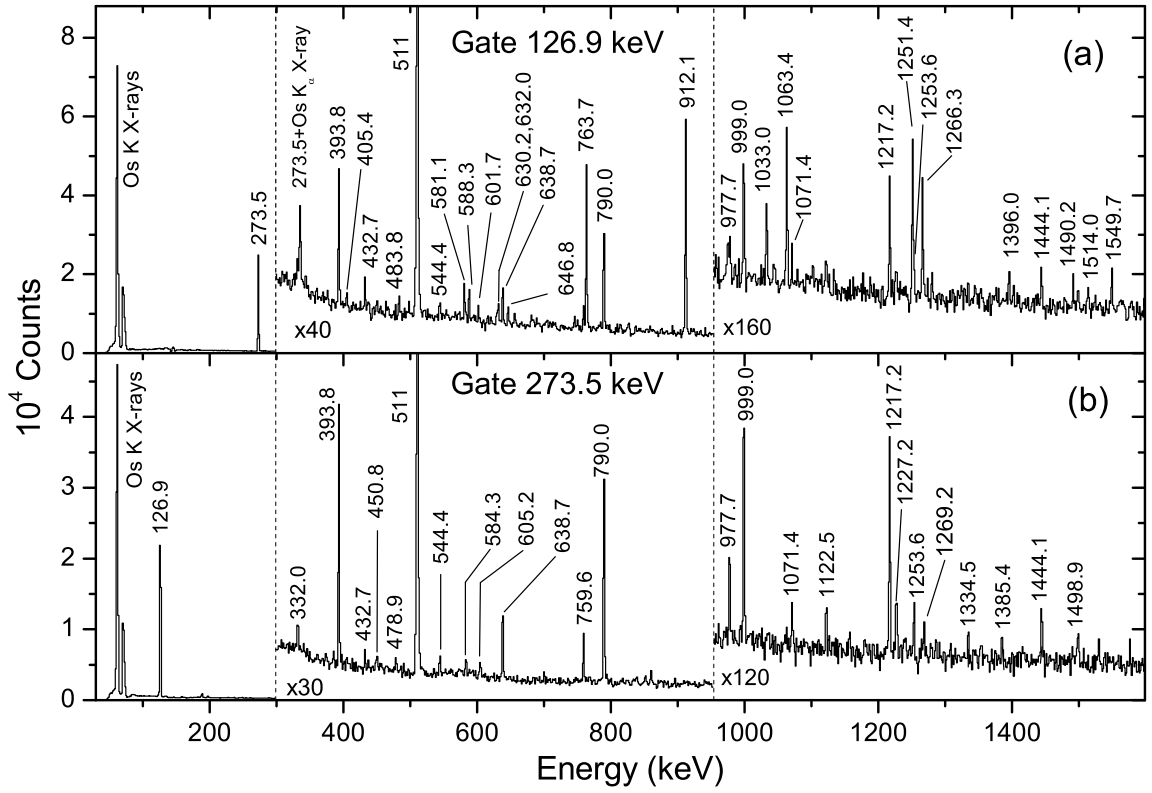

Fig. 3. γ-ray coincidence spectra gated on the (a) 126.9 keV and (b) 273.5 keV γ-rays belonging to the ^{182}Ir $\rightarrow$ ^{182}Os decay.

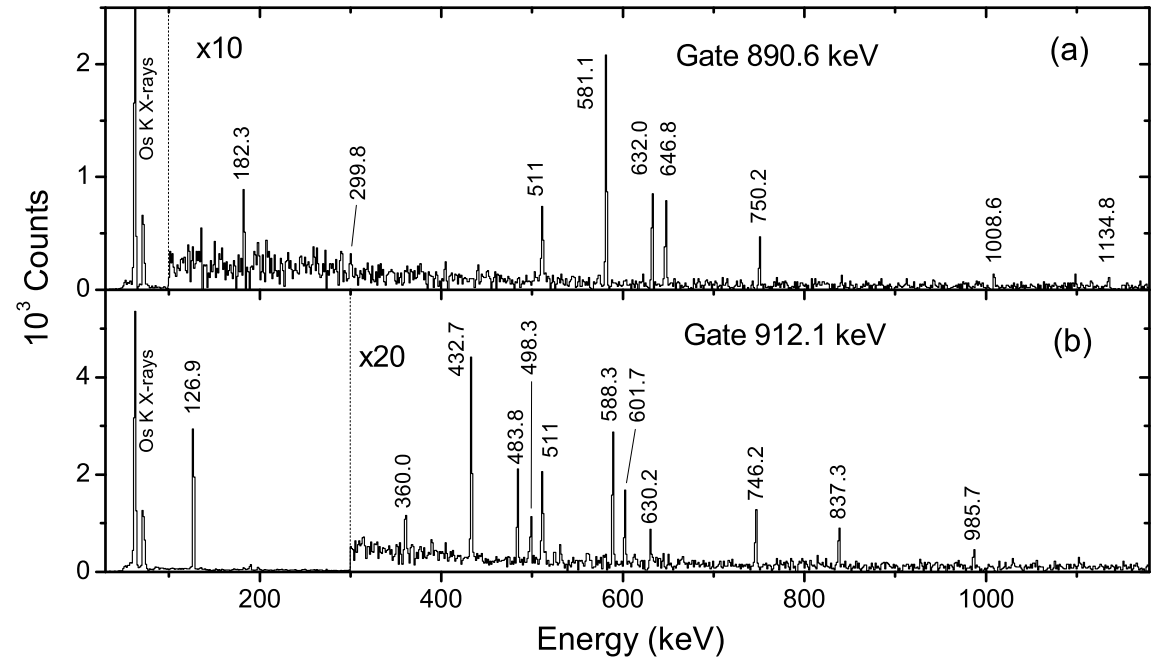

Fig. 4. γ-ray coincidence spectra gated on the (a) 890.6 keV and (b) 912.1 keV γ-rays belonging to the ^{182}Ir $\rightarrow$ ^{182}Os decay.

Table 2. Total intensity balance for the 2^+ and 4^+ states of ^{182}Os ground-state band, and Log ft values for the β^+/EC transitions to these states.

Level energy (keV)	I^π	$\gamma + e^-$ feeding	De-excitation	β^+/EC feeding (%)	Log ft
126.9	2^+	53(2)	94(4)	≤ 47	≥ 6.47
400.4	4^+	13(2)	35(1)	≤ 25	≥ 6.65

The total intensity balances at the 2^+ and 4^+ members of the ground-state band are consistent with strong direct β^+/EC decay feedings to these levels (table 2). It has to be noted that the $\gamma+e^-$ feedings reported in table 2 correspond to lower limits (there could be unseen feeding transitions) and therefore we were only able to extract upper limits for the direct β^+/EC decay feedings. Table 2 presents also lower limits of the Log ft values for the β^+/EC decay branches to both states. These Log ft values were calculated with the LOGFT code [17] using $Q = 5557(30)$ keV [18] and $T_{1/2} = 15(1)$ m [4] and assuming no direct feeding for the ground state. The values obtained indicate, according to the Raman and Gove rules [19], allowed $\Delta I = 1$, $\Delta\pi = +$ β transitions, which supports the $I^\pi = 3^+$ assignment for the ^{182}Ir ground state proposed in ref. [20] with the $\pi 1/2^-[541] \otimes \nu 1/2^-[521]$ structure, which implies a mixing of $K = 0$ and $K = 1$ components.

The electron and γ-ray measurements were used to extract conversion electron coefficients of several transitions of ^{182}Os. The high-energy part of the singles γ-ray spectrum and the corresponding electron spectrum are shown in figs. 5 (a) and (b), respectively. From a brief comparison of figs. 5 (a) and (b) the large K-conversion of the 977.7 and 1033.0 relative to the 999.0 and 1063.4 keV transitions is evident. Conversion electron and γ-ray intensities were normalized using the conversion coefficient of the pure $E2$ 273.5 keV transition in the K-shell. Due to the low statistics of the e^--γ coincidences, singles spectra were used in the analysis except for the case of the 912.1 keV transition. For this latter transition the K-conversion line in the singles spectra is not pure since the 914.9 keV ^{182}Ir K line has almost the same energy. To avoid this contamination a gated electron spectrum on the Os K X-rays was used in the analysis. The obtained experimental conversion coefficients are listed in table 3 and compared with theoretical values. In the case of anomalously large conversion coefficients additional information is given, as discussed below. Some data on electron conversion measurements were available in ref. [15] concerning the K-conversion of the 126.9, 393.8, 763.7, 790.0, 890.6, and 912.1 keV transitions, but no $E0$ components were reported.

Unique spin and parity indicated without parenthesis in figs. 1 and 2 have been taken from previous works [2, 4]. The level at 1393.2 keV is assigned as (2^+) because of the 1266.2 keV line and the two tentative 993.3 and 1393.1 keV transitions depopulating this level into the 2^+, 4^+ and 0^+ states of the ground state band, respectively. In addition, a possible $E0$ part in the 1266.2 keV transition is compatible with this assignment (see below). The level at 1617.4 keV has spin $I^\pi = 3^+, 4^+$ because of the observed connections with the 2^+ and 4^+ states and the experimental conversion coefficient extracted for the 1217.2 keV transition, compatible with $M1$ or $E0+(M1)+E2$ multipolarities. The five observed transitions depopulating the new observed state at 1669.4 keV fix unambiguously the spin and parity $I^\pi = 4^+$ of this level. For several states which have uncertainty both in the spin and the parity no assignment is indicated in the level scheme. Transition multipolarities, in the case they are unambiguously established ([2,4] and this work), are indicated in the level scheme (figs. 1 and 2).

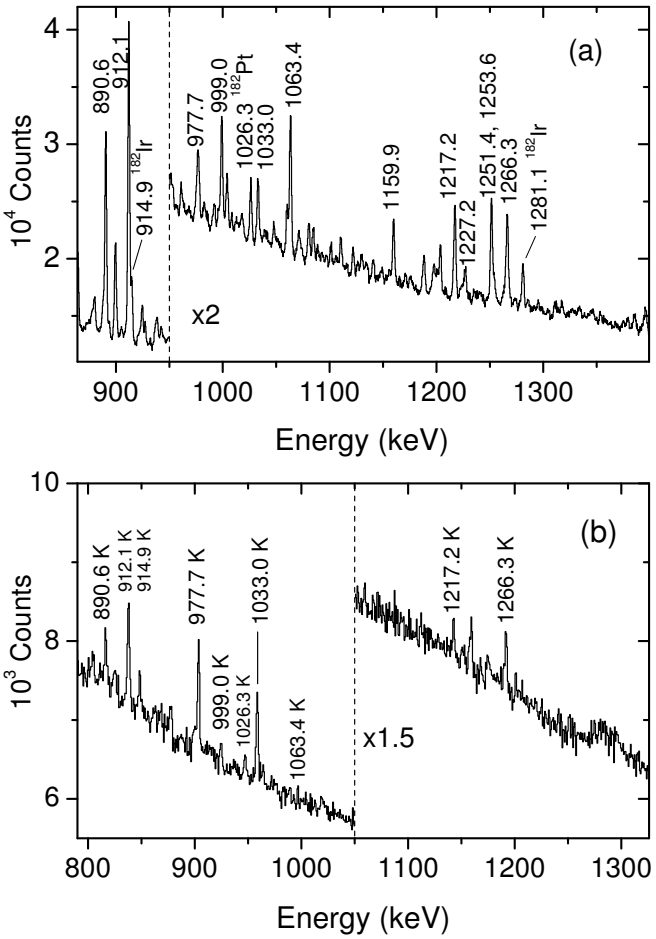

Fig. 5. High-energy section of the (a) γ-ray and (b) electron singles spectra corresponding mainly to the ^{182}Ir $\rightarrow$ ^{182}Os decay.

4 Discussion

The anomalously large experimental conversion coefficients measured for several transitions, higher than that expected for $E2$ and $M1$ transitions, provide information about the multipolarities of the transitions and the ΔI and $\Delta\pi$ values between the corresponding initial and final

Table 3. Conversion electron data and multipolarities for some transitions in ^{182}Os. The third column contains the experimental internal conversion coefficients (ICC_{exp}) or the indicated ratio and columns 4-6 the corresponding theoretical values (ICC_{th} or ratio). For some transitions with assigned $E0$ components, the $\delta(E2/M1)$ values, the $E0/E2$ mixing ratios for the K-shell (for $\lambda = 0$) ($q^2(E0/E2)$), and the ratios of the $E0$ and $E2$ strengths ($X(E0/E2)$) are reported.

E_γ	Type	ICC_{exp}	ICC^a_{th} or ratio			$\delta(E2/M1)^b$	$q^2(E0/E2)$	$X(E0/E2)$	Multipolarity
(keV)		or ratio	$E1$	$E2$	$M1$				
126.9	$\alpha_{L_{1,2}}$	0.48(6)	0.0247	0.531	0.390				$E2$
	α_{L_3}	0.34(4)	0.00556	0.376	0.00355				
	$\alpha_{L_{1,2}}/\alpha_{L_3}$	1.40(7)		1.41					
393.8	α_K	0.025(5)	0.0108	0.0302	0.106				$E2$
763.7	α_K	0.0095(20)	0.00272	0.00694	0.0191	-10^{+3}_{-11}	0.36(31)	0.009(8)	$E0+M1+E2$ or abnormal $M1+E2$
890.6	α_K	0.0071(15)	0.00203	0.00510	0.0130				$E2$
912.1	α_K	0.007(2)	0.00194	0.00487	0.0122				$M1+E2$
977.7	α_K	0.13(2)	0.00171	0.00425	0.0103	$-11.2^{+4.4}$	30(5)	1.24(20)	$E0+M1+E2$
999.0	α_K	≤ 0.008	0.00164	0.00407	0.00975				$M1+E2$
1033.0	α_K	0.053(8)	0.00154	0.00382	0.00897	+46	12.9(21)	0.60(10)	$E0+M1+E2$
1217.2	α_K	0.008(2)	0.00115	0.00279	0.00597		1.9(7)	0.12(5)	$E0+(M1)+E2$ or $M1$
1266.3	α_K	0.014(3)	0.00108	0.00259	0.00541		4.4(12)	0.31(8)	$E0+(M1)+E2$ or abnormal $M1+E2$

[a] ICC_{th} values were obtained using the HSICC code [13].
[b] From ref. [2].

states. Disregarding higher multipolarities which would involve long lifetimes, this fact has been used to indicate $E0$ admixtures in the transitions and, consequently, $I^\pi \to I^\pi$ decay assignments. However, since $M1$ conversion anomaly is well established in this mass region [5], this phenomenon cannot be discarded *a priori* in ^{182}Os. In order to determine the presence of $E0$ components in anomalously highly converted transitions we analyzed the experimental internal conversion coefficients in terms of mixing ratios and penetration factors. For an $I^\pi \to I^\pi$ transition with $E0+M1+E2$ multipolarity the internal conversion coefficient in the K-shell can be written as follows [21]:

$$\alpha_K(\text{exp}) = \frac{\delta^2(q^2+1)\alpha_K(E2) + \alpha_K(M1,\lambda)}{1+\delta^2} \qquad (1)$$

with

$$\alpha_K(M1,\lambda) = \alpha_K(M1)(1 + B_1(K)\lambda + B_2(K)\lambda^2), \qquad (2)$$

where $q^2 = I_{e,K}(E0)/I_{e,K}(E2)$ is the $E0/E2$ mixing ratio for the K-shell, $\delta^2 = I_\gamma(E2)/I_\gamma(M1)$ is the $E2/M1$ mixing ratio, λ is the penetration factor, $B_1(K)$ and $B_2(K)$ are the penetration coefficients which depend on the atomic number [22], and $\alpha_K(E2)$ and $\alpha_K(M1)$ are the theoretical internal conversion coefficients in the K-shell. The dimensionless ratios of the $E0$ and $E2$ transition probabilities, $X(E0/E2)$, were evaluated according to the following expression [21]:

$$X(E0/E2) = 2.56 \times 10^9 A^{4/3} E_\gamma^5 q^2 \alpha_K(E2)/\Omega_K\,,$$

where E_γ is the transition energy expressed in MeV and Ω_K is the electronic factor in s^{-1} calculated using the OMEGA.BAS program [23]. The quantities q^2, evaluated from eq. (1), assuming $\lambda = 0$, and the $X(E0/E2)$ values are listed in table 3. The δ values reported in ref. [2] were used in the calculations and when this information was not available, negligible $M1$ admixtures were assumed. The penetration factors were evaluated from eqs. (1) and (2), under the hypothesis of $M1$ conversion anomaly without monopole components. Solving the quadratic equation, extremely large absolute values of λ were obtained for the 977.7 and 1033.0 keV transitions: $|\lambda| \geq 1.5(7) \times 10^3$ and $|\lambda| \geq 4.1(4) \times 10^3$, respectively. Since high penetration factors are very rare, the largest reported one, in our knowledge, is $\lambda = 175$ in ^{181}Ta [24], we assumed that the high conversion of the 977.7 and 1033.0 keV transitions is mainly caused by an $E0$ component. For the 763.7 keV transition the experimental results are consistent with a small $E0$ component or with an anomaly in the $M1$ conversion with a penetration factor $\lambda = 193^{+269}_{-98}$ or $\lambda = -113^{+98}_{-269}$. Also large conversion coefficients were measured for the 1217.2 and 1266.3 keV transitions. Since γ-γ angular-correlation data were not available for these transitions their q^2 and $X(E0/E2)$ values reported in table 3 were obtained under the assumption that the $M1$ components are negligibly small, and hence the multipolarities are assumed to be $E0+E2$. It has to be mentioned that according to our experimental data another possible assignment for the 1217.2 keV transition might be pure $M1$ multipolarity, so the level at 1617.4 keV could have 3^+ or 4^+ spin and parity values.

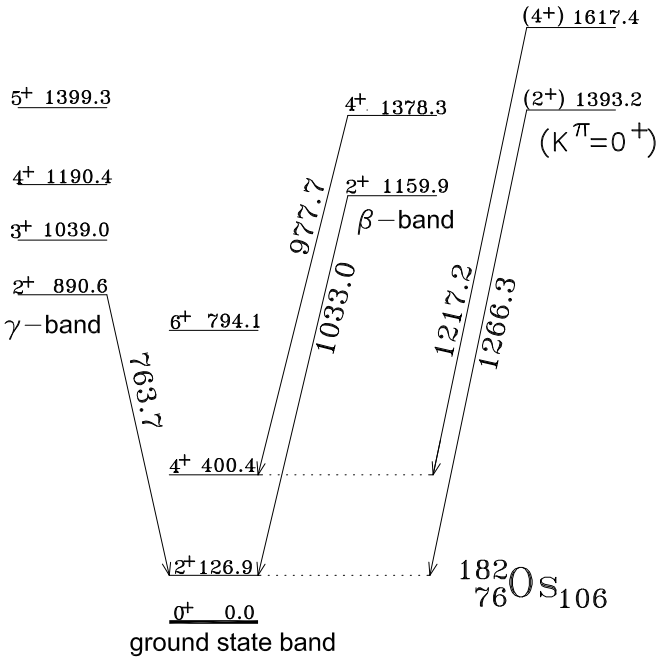

Fig. 6. Ground-state band, γ-band, β-band, and a proposed second excited $K^\pi = 0^+$ band of ^{182}Os, as observed in the present work. The transitions, for which $E0$ components were assigned, are indicated.

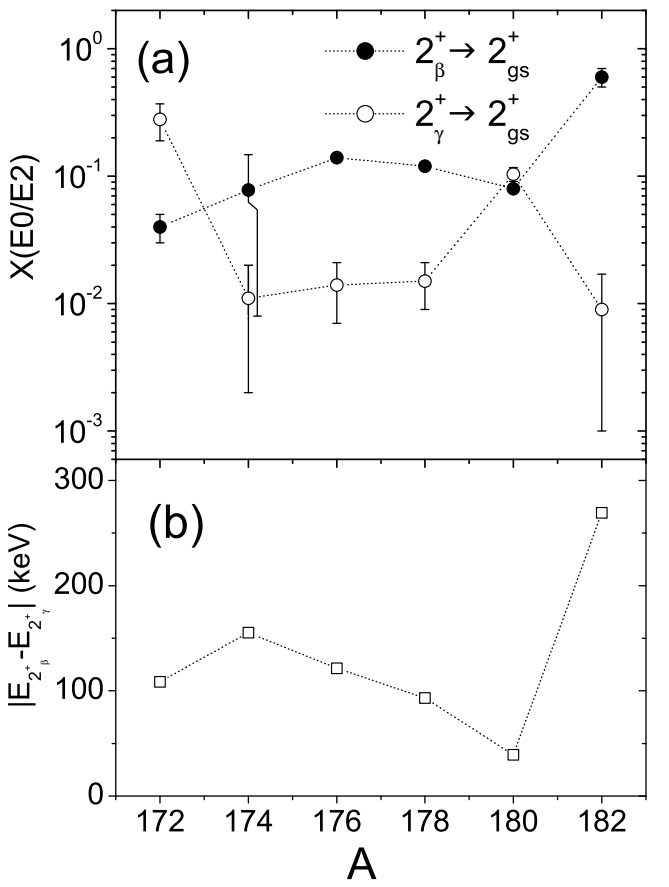

Fig. 7. Systematics of (a) the $X(E0/E2)$ strengths for the $2^+_\beta \rightarrow 2^+_{gs}$ and $2^+_\gamma \rightarrow 2^+_{gs}$ transitions and (b) the absolute energy difference between the 2^+_β and the 2^+_γ states in the $A = 172$–182 Os isotopes.

The low-spin states of ^{182}Os have been widely studied [2,4,25]. Here we will discuss some results concerning the positive-parity structures. The positive-parity low-spin levels of ^{182}Os have been interpreted in terms of rotational bands based on the deformed ground state (gs), the γ vibration (γ-band), and the first excited 0^+ state (β-band) [2,4]. We use the term β-band just as a nomenclature since the mechanism of this first excited $K^\pi = 0^+$ band is not clear, it might arise from a secondary minimum in the potential energy as well as from a β vibration. These excitations are shown in fig. 6 together with selected interband transitions. The identification of the levels at 1159.9 and 1378.3 keV as the 2^+ and the 4^+ states of the β-band [2] is compatible with the observed decays into the ground-state band and with the strong $E0$ components of the 1033.0 and 977.7 keV transitions. From the results shown in table 3, it can be observed that the largest $X(E0/E2)$ ratios correspond to these transitions between the β- and the ground-state bands, both $K^\pi = 0^+$ bands. Figure 6 also displays two new levels at 1393.2 and 1617.4 keV which are tentatively interpreted as the (2^+) and (4^+) members of a possible second excited $K^\pi = 0^+$ band. From the two possible spin-parity assignments reported in the level scheme (fig. 1) we adopted $I^\pi = (4^+)$ for the 1617.4 keV state. In addition, the energy spacing between these (2^+) and (4^+) states of 224.2 keV corresponds to a reasonable deformation for a $K^\pi = 0^+$ band. Similar bands established from the 0^+ state have been reported in ^{178}W [1] and in ^{176,178}Hf [26,27]. The non-observation of the 0^+ states of the β-band and also of this proposed second excited $K^\pi = 0^+$ band is due to the negligible population of the 0^+ levels directly by beta decay involving second forbidden-unique transitions and also the expected negligible branching for the de-excitations inside the bands (see below). Assuming that the high conversion of the 763.7 keV transition linking the γ- and the ground-state band is due to an $E0$ component its corresponding $X(E0/E2)$ ratio follows the systematics of these ratios for the $2^+_\gamma \rightarrow 2^+_{gs}$ transitions in neighboring nuclei [1,2]. An $E0$ component in this transition would evidence a band mixing, since $E0$ transitions are forbidden between $K^\pi = 0^+$ and $K^\pi = 2^+$ pure states [2]. In fig. 7(a) the $X(E0/E2)$ ratios for the $2^+_\beta \rightarrow 2^+_{gs}$ and $2^+_\gamma \rightarrow 2^+_{gs}$ transitions are represented for the Os isotopes ([2,28] and present work). As already mentioned in ref. [2] the 2^+_β and 2^+_γ states in ^{180}Os are only 39.3 keV apart and consequently their wave functions are expected to be highly mixed. Contrary, in ^{182}Os the larger distance of 269.3 keV between these levels corresponds to states weakly mixed. In fig. 7(b) the energy distance between the 2^+_β and 2^+_γ states is plotted for the Os isotopes. The correlation between the $X(E0/E2)$ ratios for the $2^+_\gamma \rightarrow 2^+_{gs}$ transitions of fig. 7(a) and the energy distances of fig. 7(b) is clearly observed, roughly both quantities evolve with the mass

Table 4. Analysis of the $B(E2)$ values and comparisons of the experimental results with the Alaga rule predictions for the transitions of the β-band into the ground-state band in ^{182}Os.

$\frac{I_\beta \to I_{gs}}{I_\beta \to I'_{gs}}$	$\frac{B(E2, I_\beta \to I_{gs})}{B(E2, I_\beta \to I'_{gs})}$	
	exp.	Alaga
$\frac{2_\beta \to 0_{gs}}{2_\beta \to 4_{gs}}$	0.17(2)	0.39
$\frac{2_\beta \to 2_{gs}}{2_\beta \to 4_{gs}}$	0.28(2)	0.56
$\frac{4_\beta \to 2_{gs}}{4_\beta \to 6_{gs}}$	0.14(3)	0.63
$\frac{4_\beta \to 4_{gs}}{4_\beta \to 6_{gs}}$	0.12(3)	0.57

number displaying opposite slope, when one quantity increases the other one decreases and vice versa. On the other hand, the larger energy distance between the 2^+_γ and 2^+_{gs} of about 0.7 MeV remains fairly constant along the Os isotopes implying a smaller and constant mixing between the 2^+_γ and 2^+_{gs} states. Therefore, the evolution of the $X(E0/E2)$ ratios for the $2^+_\gamma \to 2^+_{gs}$ transitions with the mass number could be explained mainly in terms of the mixing between the β and γ excitations in the 2^+_γ state.

The ratios of the $B(E2)$ values for the decays of the β-band into the ground-state band were evaluated and compared with the predictions of the Alaga rule. According to this rule the relative transition probabilities are given by the Clebsch-Gordan coefficients only:

$$\frac{B(E2, I_\beta \to I_{gs})}{B(E2, I_\beta \to I'_{gs})} = \frac{\langle I_\beta 020 | I_{gs} 0\rangle^2}{\langle I_\beta 020 | I'_{gs} 0\rangle^2}\,.$$

As can be seen in table 4 all the experimental values fall below the theoretical expectations. For the transitions decaying from the 2^+_β state the ratios ($\frac{2_\beta \to 0_{gs}}{2_\beta \to 4_{gs}}$ and $\frac{2_\beta \to 2_{gs}}{2_\beta \to 4_{gs}}$) follow the general trend of the systematics for the Sm-W nuclei with neutron numbers N = 90–110, presented in ref. [6], where the majority of the data lies below the Alaga predictions. Garret [6] suggested that these deviations from the Alaga rule may indicate that the branchings are in error or that the mixings have altered the $B(E2)$ significantly. In the next section we will show theoretical results obtained in the framework of a microscopic configuration mixing approach and compare them with the available experimental data in Os isotopes.

4.1 Theoretical calculations within a microscopic dynamical approach

At this stage of the discussion, in order to attempt to answer the still open questions, it is interesting to compare the experimental results to the theoretical predictions obtained in the framework of a microscopic model that

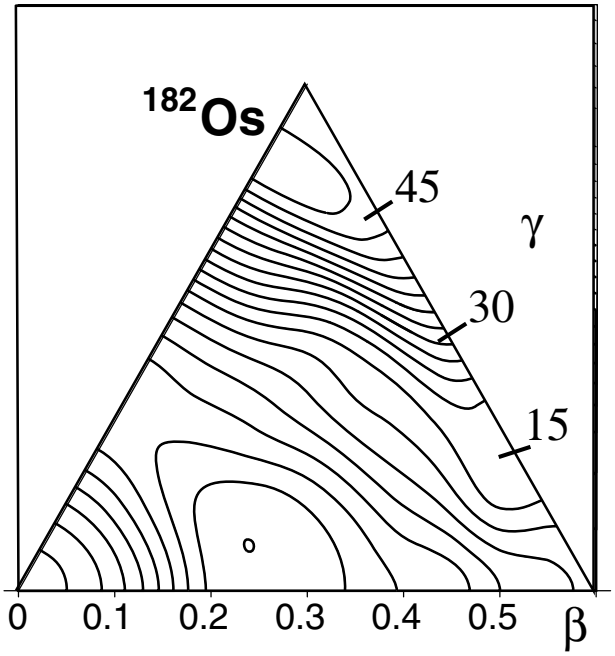

Fig. 8. Potential energy surface $V(\beta, \gamma)$ predicted for ^{182}Os using the constrained HFB calculations.

remains free of adjustable parameters. Considering long-range correlations beyond the Hartree-Fock-Bogoliubov (HFB) mean-field approach implemented with the D1S Gogny force [8], we have used here a full quadrupole Generator Coordinate Method under Gaussian Overlap Approximation (GCM-GOA) that has been applied at large scale in different regions of the nuclear chart, for instance, in ref. [29]. This approach is expected to provide a rather good description of deformed nuclei. In this framework, constrained HFB calculations are performed under quadrupole axial and triaxial constraints to map against deformation variables β and γ, the constitutive elements (potential energy surface, moments of inertia and kinetic vibrational masses) of the resulting five-dimensional collective Hamiltonian which describes on the same ground, vibrational and rotational motions. Eigenstates of the collective Hamiltonian are finally expressed as normalized combinations of the form:

$$\Psi^{I\alpha} = \sum_{K even \geq 0} A^{I\alpha}_K(\beta, \gamma)\varphi^{IM}_K(\Omega),$$

where $\varphi^{IM}_K(\Omega)$ is the standard combination of Wigner rotation matrices, α the state number, I the angular momentum, K and M the I projection on the third axis in intrinsic and laboratory frames, respectively. In what follows, we will call "K-component" of the $\Psi^{I\alpha}$ wave functions the quantity:

$$a^2_K = \int |A^{I\alpha}_K(\beta, \gamma)|^2 \mu \mathrm{d}\beta \mathrm{d}\gamma, \qquad (3)$$

where $\mu \mathrm{d}\beta \mathrm{d}\gamma$ is the metric. Equation (3) obviously verifies

$$\sum_{K even \geq 0} a^2_K = 1.$$

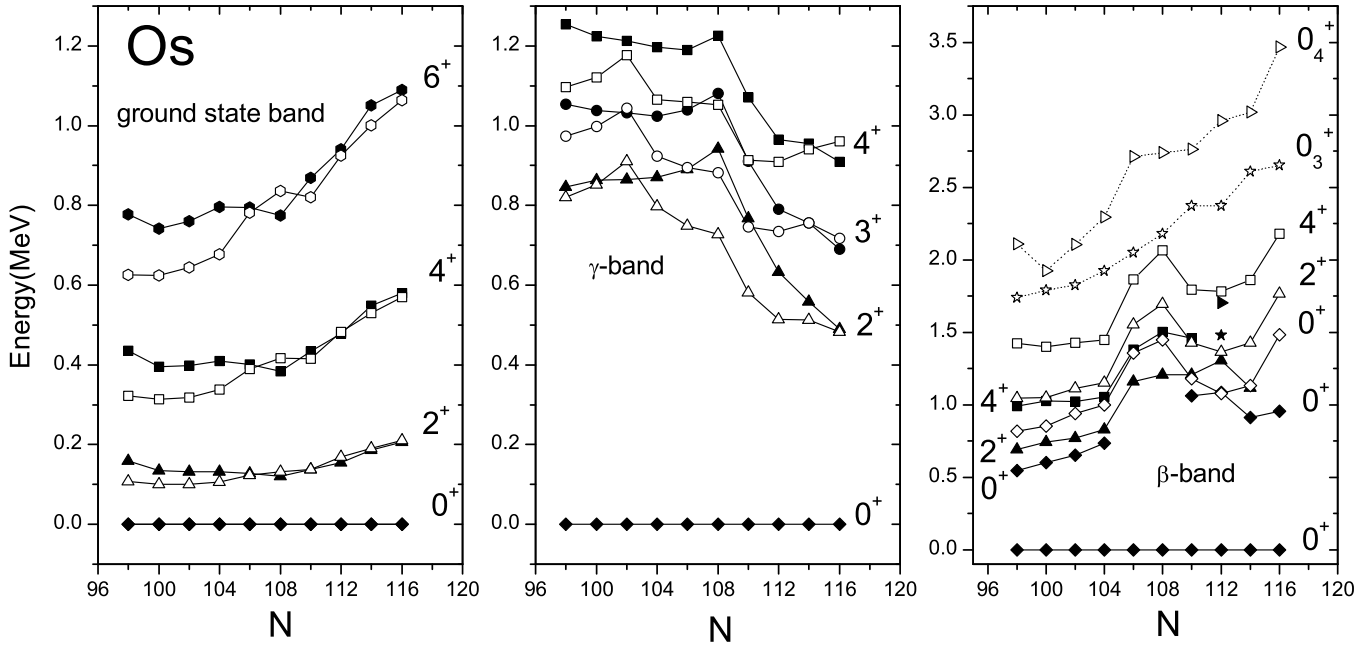

Fig. 9. Experimental (full symbols) and predicted (open symbols) low-lying collective levels for the ground-state, γ- and β-bands of the even-even $^{174-192}$Os nuclei. The calculated 0_3^+ and 0_4^+ states are shown on the right-hand-side part of the figure.

In the following, the β_{min} and γ_{min} are the deformation parameters at the minimum of the potential energy surfaces, they are the "static" deformations. The β_{rms} and γ_{rms} are the root mean square deformation parameters calculated for each excited state; they take into account dynamical effects. For more details in the theoretical treatment, see ref. [29] and references therein.

4.1.1 Theoretical results

Calculations have been performed for the even-even $^{174-192}$Os nuclei. The potential energy surface of ^{182}Os is shown in fig. 8 as an example. It exhibits only one minimum for $\beta_{min} = 0.243$ and $\gamma_{min} = 11.3°$, *e.g.*, rather on the prolate side. On the oblate edge the local minimum is only around 2.5 MeV above the prolate one. That means that we expect for ^{182}Os the behavior of a rather soft nucleus. The low-lying collective levels predicted for $^{174-192}$Os are displayed as open symbols in fig. 9 where they have been classified into ground-state, γ- and β-bands, using their wave function properties. They are compared with the experimental results shown as full symbols. On the right-hand-side part of fig. 9 that presents the β-band, 0_3^+ and 0_4^+ states have also been reported. We can note that the energy evolution of the levels of the three bands is generally rather well reproduced by the calculations. For the ground-state band, the agreement is perfect for $N \geq 106$, whereas farther from stability, the states are predicted to be located at slightly too low energies. For the γ-band, the states are calculated at too low energies for $102 < N < 114$, but the agreement is very good for $N < 104$ and $N > 112$. For ^{182}Os ($N = 106$), the energy difference between the predicted and observed levels is around 150 keV. As for the β-band the levels are calculated at too high energies. On the other hand, their energy evolution with N is perfectly reproduced. The 0_3^+ and 0_4^+ states are only observed in ^{188}Os ($N = 112$), they are located at much lower energies than that expected from the calculations. The $B(E2)$ and $\rho(E0)$ values have been calculated using the standard collective model formulas as defined, for instance, in ref. [30]. The $B(E2)$ values of the $2_{gs}^+ \rightarrow 0_{gs}^+$ transitions in the $^{174-192}$Os nuclei are compared with the calculated ones in fig. 10. The theoretical values are maximal for ^{176,178}Os. Unfortunately, the corresponding experimental values are missing and the values for ^{174,180}Os have large error bars. It is worth noting that the model slightly overestimates the $B(E2)$ values. Nevertheless, a satisfactory agreement is obtained since the known $B(E2)$ values are reproduced within 40% except for that of ^{180}Os. The $\rho(E0)$ and $X(E0/E2)$ values determined for the five highly converted transitions of ^{182}Os are reported in table 5. The $X(E0/E2)$ values are compared with the experimental ones in fig. 11. The agreement is rather good for the $2_\beta^+ \rightarrow 2_{gs}^+$ and $4_\beta^+ \rightarrow 4_{gs}^+$ transitions for which the high conversion coefficients have been shown to be mainly due to an $E0$ component. The theoretical values are slightly smaller than the experimental ones but we have to keep in mind that the $B(E2)$ values are slightly overestimated by the model for the $2_{gs}^+ \rightarrow 0_{gs}^+$ transitions (see fig. 10). If this overestimation is also true for the $2_\beta^+ \rightarrow 2_{gs}^+$ and $4_\beta^+ \rightarrow 4_{gs}^+$ transitions, then the $X = B(E0)/B(E2)$ values are expected to be slightly underestimated. An $M1$ and $E0$ contributions being forbidden for the $\Delta K = 2$ $2_\gamma^+ \rightarrow 2_{gs}^+$ transition, an $E0$ part can only be due to the presence of a $K = 0$ component in the wave function of the 2_γ^+ state. We can see in ta-

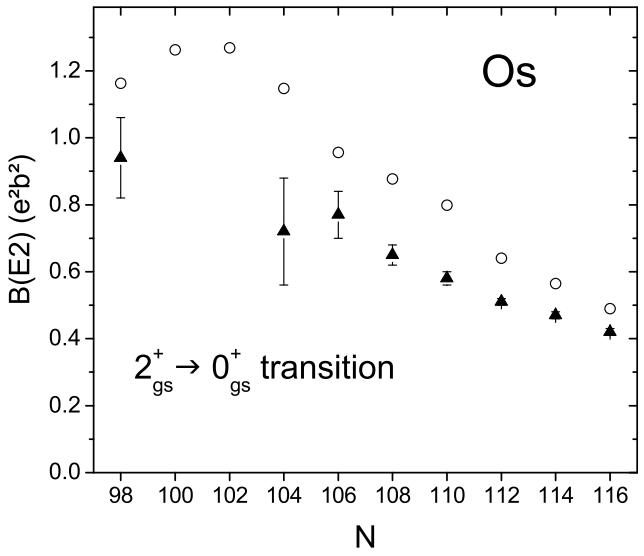

Fig. 10. Experimental (full symbols) and predicted (open symbols) $B(E2)$ values of the $2^+_{gs} \rightarrow 0^+_{gs}$ transitions in the even-even $^{174-192}$Os nuclei.

Table 5. The calculated $\rho(E0)$ and $X(E0/E2)$ values corresponding to $\Delta I = 0$, and $\Delta\pi = +$ transitions of ^{182}Os.

Transition	$\rho(E0)$	$X(E0/E2)$
$2^+_\gamma \rightarrow 2^+_{gs}$	−0.0088	0.0000999
$2^+_\beta \rightarrow 2^+_{gs}$	−0.193	0.207
$4^+_\beta \rightarrow 4^+_{gs}$	−0.202	0.268
$2^+_5 \rightarrow 2^+_{gs}$	−0.0983	0.895
$4^+_6 \rightarrow 4^+_{gs}$	+0.0718	3.16
$2^+_4 \rightarrow 2^+_{gs}$	−0.0542	0.827
$4^+_5 \rightarrow 4^+_{gs}$	−0.0658	2.56

ble 6 that the $K = 0$ component calculated for the 2^+_γ state is very small, which means that it cannot be precisely determined. Moreover, for the $2^+_\gamma \rightarrow 2^+_{gs}$ transition, the existence of an anomalous $M1$ contribution cannot be ruled out. The 0^+_3, 2^+_5 and 4^+_6 states of the second excited $K = 0$ band of ^{182}Os are calculated at 2.050, 2.303 and 2.676 MeV, respectively, whereas the 2^+ and 4^+ states of the proposed second excited $K = 0$ band are located at only 1.393 and 1.617 MeV. Besides this, an excited band, 2^+_4 and 4^+_5 states with main $K = 2$ component are calculated at lower energies, namely 1.996 and 2.378 MeV, respectively. The $X(E0/E2)$ values calculated for the $2^+_5 \rightarrow 2^+_{gs}$ and $2^+_4 \rightarrow 2^+_{gs}$ transitions and those obtained for the $4^+_6 \rightarrow 4^+_{gs}$ and $4^+_5 \rightarrow 4^+_{gs}$ transitions are very similar. They are shown in fig. 11 as open triangles for the transitions involving the mainly $K = 0$ states and as stars for the transitions involving the mainly $K = 2$ states. The K-components (see eq. (3)) of these 2^+_4, 2^+_5, 4^+_5 and 4^+_6 states wave functions are given in table 6. The admixture in these wave functions is relatively

Table 6. Predicted deformation, energy, and wave function components for states of ^{182}Os.

State	β_{rms}	γ_{rms} (°)	Energy (MeV)	K-Components (%)		
				$K = 0$	$K = 2$	$K = 4$
0^+_{gs}	0.268	14.8	0.0	100		
2^+_{gs}	0.270	14.3	0.123	99.84	0.16	
4^+_{gs}	0.274	13.8	0.390	98.92	1.07	0.01
2^+_γ	0.265	20.1	0.749	0.44	99.56	
4^+_γ	0.272	18.8	1.059	2.10	97.11	0.79
0^+_β	0.275	21.6	1.357	100		
2^+_β	0.286	18.4	1.552	96.63	3.37	
4^+_β	0.295	16.2	1.864	92.65	5.08	2.27
2^+_4	0.276	25.3	1.996	12.34	87.66	
0^+_3	0.285	22.4	2.050	100		
2^+_5	0.286	21.2	2.303	89.16	10.84	
4^+_5	0.286	22.7	2.378	26.29	64.46	9.25
4^+_6	0.292	20.3	2.676	70.78	29.06	0.16
0^+_4	0.287	23.5	2.711	100		

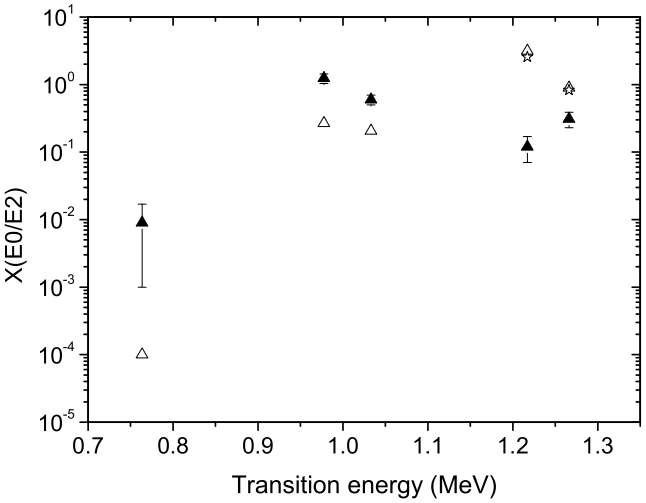

Fig. 11. Experimental (full symbols) and predicted (open symbols) $X(E0/E2)$ values for the five highly converted transitions of ^{182}Os.

important, which is due to their energy location that is rather high. This can explain why the $X(E0/E2)$ values are so close in spite of the different K values of their dominant K-component. Therefore, the calculations do not allow us to firmly conclude as for the structure $K = 0$ or $K = 2$ of the band proposed as the second excited $K^\pi = 0^+$ band in fig. 6. To illustrate the softness of the ^{182}Os nucleus, the β_{rms} and γ_{rms} deformation parameters of every nuclear states are also reported in table 6. In order to analyze why the band head of the β-band is not observed in ^{182}Os, whereas it has been seen in ^{188}Os, we have calculated the $PE2(2^+_\beta \rightarrow 0^+_\beta)/PE2(2^+_\beta \rightarrow 0^+_{gs})$ and $PE2(2^+_\beta \rightarrow 0^+_\beta)/PE2(2^+_\beta \rightarrow 2^+_{gs})$ transition probability ratios for ^{188}Os and ^{182}Os. For the energy of the

Table 7. Transition probability ratios in ^{182,188}Os.

Transition probability ratio	^{182}Os	^{188}Os
$PE2(2^+_\beta \to 0^+_\beta)/PE2(2^+_\beta \to 0^+_{gs})$	2.44×10^{-4}	3.51×10^{-2}
$PE2(2^+_\beta \to 0^+_\beta)/PE2(2^+_\beta \to 2^+_{gs})$	2.38×10^{-4}	1.93×10^{-2}

Table 8. Comparisons of experimental ratios of $B(E2)$ strengths with the theoretical predictions in ^{182}Os.

$\frac{I_i \to I_f}{I_i \to I_{f'}}$	$\frac{B(E2, I_i \to I_f)}{B(E2, I_i \to I_{f'})}$	
	exp.	theory
$\frac{2_\beta \to 0_{gs}}{2_\beta \to 2_{gs}}$	0.61(4)	0.55
$\frac{2_\beta \to 0_{gs}}{2_\beta \to 4_{gs}}$	0.17(2)	0.18
$\frac{2_\beta \to 2_{gs}}{2_\beta \to 4_{gs}}$	0.28(2)	0.33
$\frac{4_\beta \to 2_{gs}}{4_\beta \to 6_{gs}}$	0.14(3)	0.18
$\frac{4_\beta \to 4_{gs}}{4_\beta \to 6_{gs}}$	0.12(3)	0.27
$\frac{4_\beta \to 2_\beta}{4_\beta \to 2_{gs}}$	≤ 258	71
$\frac{4_\beta \to 2_\beta}{4_\beta \to 4_{gs}}$	≤ 323	47
$\frac{4_\beta \to 2_\beta}{4_\beta \to 6_{gs}}$	≤ 43	13
$\frac{2_\gamma \to 2_{gs}}{2_\gamma \to 0_{gs}}$	2.2(1)	3.1
$\frac{4_\gamma \to 2_{gs}}{4_\gamma \to 2_\gamma}$	0.021(4)	0.017
$\frac{4_\gamma \to 4_{gs}}{4_\gamma \to 2_\gamma}$	0.17(3)	0.32

$2^+_\beta \to 0^+_\beta$ transition of ^{182}Os we used 101.3 keV assuming the same E^+_4/E^+_2 ratio in the β- and ground-state bands. The obtained values, reported in table 7, show that the 0^+_β feeding in ^{182}Os is around hundred times smaller than that in ^{188}Os, which explains why the 0^+_β of ^{182}Os has not been observed in this work. Eleven ratios of reduced transition probabilities $B(E2)$ calculated for the transitions linking the levels of the γ-, β-, and ground-state bands are listed in table 8 together with the corresponding experimental results. One can see that the results are very well reproduced for eight of them. Only upper limits have been obtained for the three ratios of the $B(E2)$ value of the $4^+_\beta \to 2^+_\beta$ intra-band transition over the $B(E2)$ values of the transitions de-exciting the 4^+_β to the levels of the ground-state band.

5 Summary

New results on low-spin states of ^{182}Os have been established from β^+/EC decay measurements using γ-ray and electron conversion spectroscopy techniques. In total 81 transitions have been located in the level scheme and 18 new levels established. Evaluation of the direct β^+/EC decay feedings and Log ft for the 2^+ and 4^+ states of the ground-state band are compatible with the structure and spin parity assignment of the ground state of the parent ^{182}Ir nucleus. Monopole admixtures in several decays of the β- and γ-bands were determined and compared with the available experimental results along the Os isotopes.

A microscopic dynamical model without any adjustable parameter, grounded on the Gogny D1S nucleon-nucleon effective interaction, has been used to study collective states and decay properties in $^{174-192}$Os. General trends of the first collective state energies are fairly well reproduced. Moreover, this model fits quite well a variety of ratios of electromagnetic values measured in ^{182}Os and allows us to explain why the first 0^+ excited state is not observed in this nucleus. On the other hand, we were not able to assign firmly the main K-component for the new levels at 1393.2 and 1617.4 keV decaying into the ground-state band by highly converted transitions that could be due to abnormal $M1$ coefficients as well as to $E0$ contributions. Under the used hypotheses (in particular the Inglis-Belyaev approximated evaluation of the vibrational mass tensor), β- and γ- bandheads should be predicted at somewhat too high energies. This is clearly the case for the 0^+ β-bandheads over the whole region. Besides this, the present model has served to show the γ softness character of the Os nuclei. In this context, it should be noticed that simple approaches as Alaga rules, which do not take into account rotation-vibration correlations, are not suitable to describe the branching ratios. Furthermore, for such soft nuclei, effects out of the model content, as other collective modes and two-quasiparticle degrees of freedom, may affect the low-energy collective spectrum and explain in particular the slight overestimation obtained for the $E2$ transition rates. Finally, we can conclude that a satisfactory agreement between measured and calculated spectroscopic properties in Os nuclei has been obtained.

References

1. T. Kibédi *et al.*, Nucl. Phys. A **688**, 669 (2001).
2. T. Kibédi *et al.*, Nucl. Phys. A **567**, 183 (1994).
3. P.M. Davidson *et al.*, Nucl. Phys. A **657**, 219 (1999).
4. B. Singh, R.B. Firestone, Nucl. Data Sheets **74**, 383 (1995).
5. B. Roussière *et al.*, Nucl. Phys. A **548**, 227 (1992).
6. P.E. Garret, J. Phys. G **27**, R1 (2001).
7. R.F. Casten, P. von Brentano, Phys. Rev. C **50**, R1280 (1994).
8. J. Dechargé, D. Gogny, Phys. Rev. C **21**, 1568 (1980); J.-F. Berger *et al.*, Nucl. Phys. A **428**, 23c (1984).
9. J.C. Putaux *et al.*, Nucl. Instrum. Methods **186**, 321 (1981).

10. P. Paris *et al.*, Nucl. Instrum. Methods **186**, 91 (1981).
11. E. Kugler, Hyperfine Interact. **129**, 23 (2000).
12. J. Lettry *et al.*, Nucl. Instrum. Methods B **126**, 170 (1997).
13. HSICC code, National Nuclear Data Center, Brookhaven National Laboratory, USA.
14. M. Finger *et al.*, CERN-70-29 (1970).
15. J.P. Husson, Thesis, University of Paris (1972), FRNC-TH-355 (1972).
16. A.I. Akhmadzhanov *et al.*, Phys. Ser. **36**, 1821 (1973).
17. LOGFT code, National Nuclear Data Center, Brookhaven National Laboratory, USA.
18. G. Audi *et al.*, Nucl. Phys. A **729**, 3 (2003).
19. S. Raman, N.B. Gove, Phys. Rev. C **7**, 1995 (1973).
20. J. Sauvage *et al.*, Nucl. Phys. A **592**, 221 (1995).
21. A.V. Aldushchenkov, N.A. Voinova, Nucl. Data Tables A **11**, 299 (1972).
22. R.S. Hager, E.C. Seltzer, Nucl. Data Tables A **6**, 1 (1969).
23. J. Kantele, *Handbook of Nuclear Spectrometry* (Academic Press, 1995).
24. E. Seltzer, R. Hager, *Proceedings of the International Conference Internal Conversion Process*, edited by J.H. Hamilton (Academic Press, Inc., New York, 1966) p. 309.
25. C. Fahlander, G.D. Dracoulis, Nucl. Phys. A **375**, 263 (1982).
26. E. Browne, H. Junde, Nucl. Data Sheets **84**, 337 (1998).
27. E. Browne, Nucl. Data Sheets **72**, 221 (1994).
28. P.M. Davidson *et al.*, Nucl. Phys. A **568**, 90 (1994).
29. J.-P. Delaroche *et al.*, Phys. Rev. C **50**, 2332 (1994); J. Libert *et al.*, Phys. Rev. C **60**, 054301 (1999); J.-P. Delaroche *et al.*, Nucl. Phys. A **771**, 103 (2006) and references therein.
30. K. Kumar, M. Baranger, Nucl. Phys. A **92**, 608 (1967).